

OVERFLOW Simulations of MSL Ballistic Range Model

13th Symposium on Overset Composite
Grids and Solution Technology
October 17-21, 2016

Darby Vicker

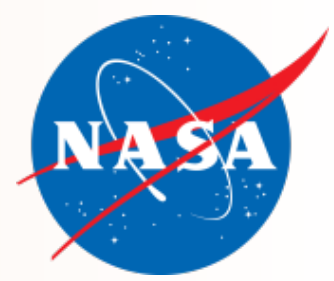
darby.vicker@nasa.gov

Alan Schwing

alan.schwing@nasa.gov



Outline



JSC/EG3 Overview and Current Work

Introduction

Grid Generation

- CGT Scripts and DCF
- Grid Sensitivity and Shock Capturing

OVERFLOW Inputs

Static Results

- Integrated Aerodynamics

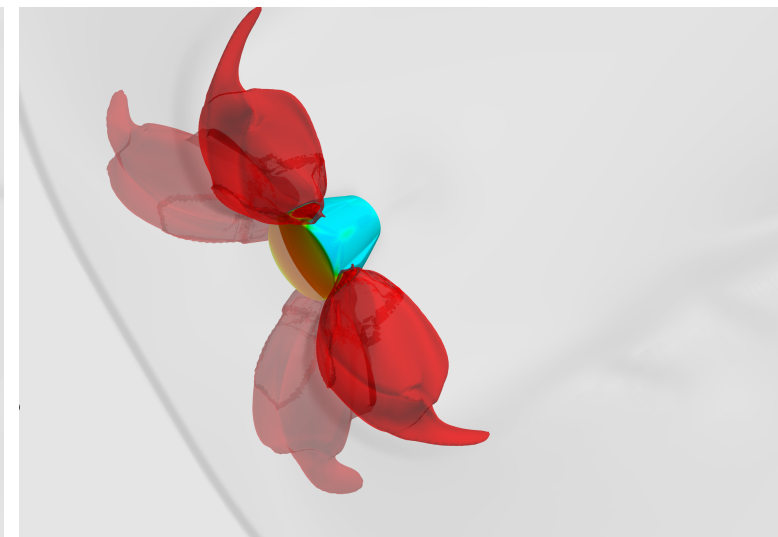
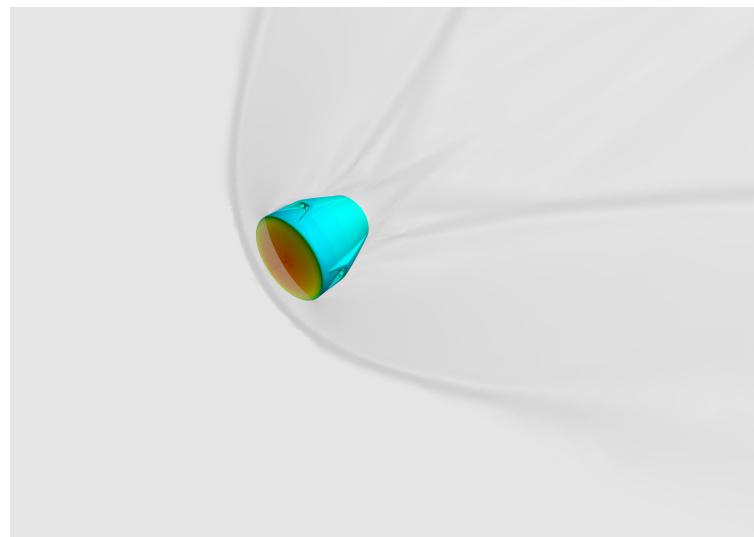
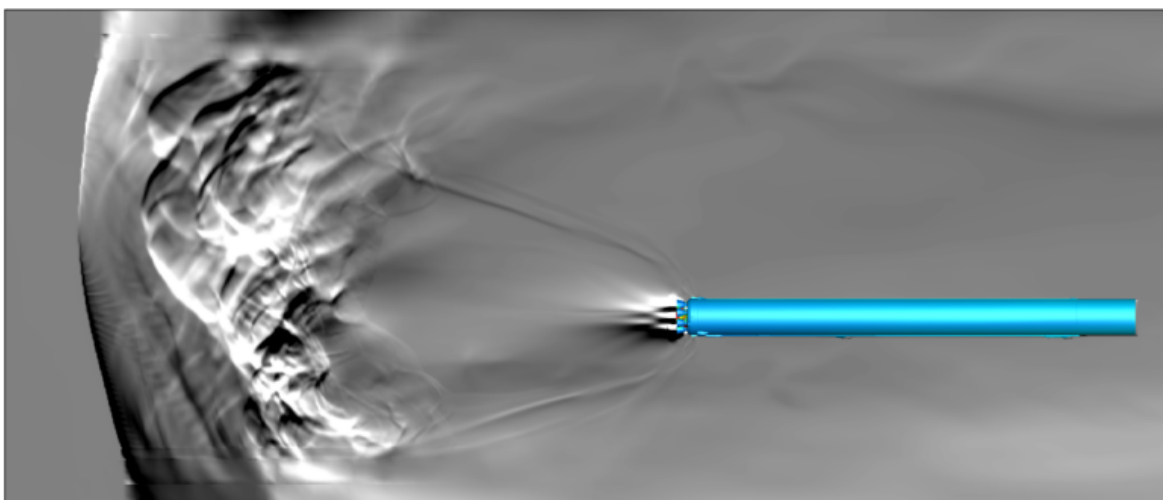
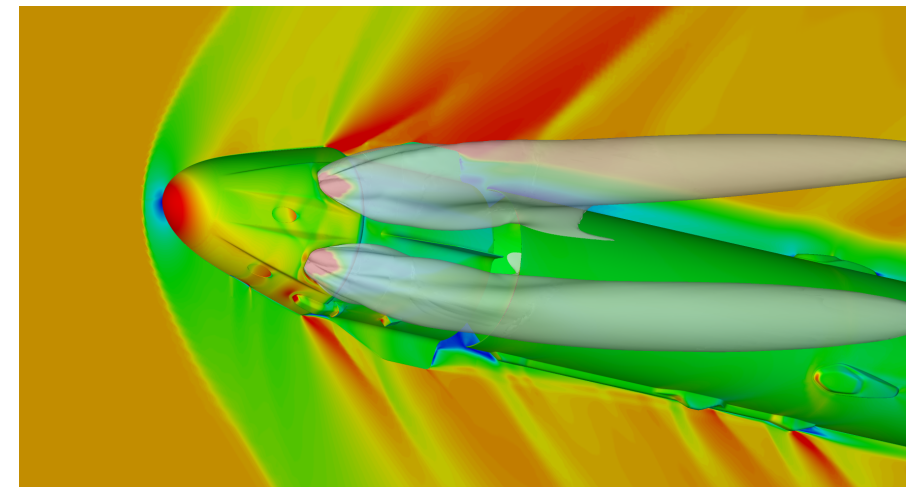
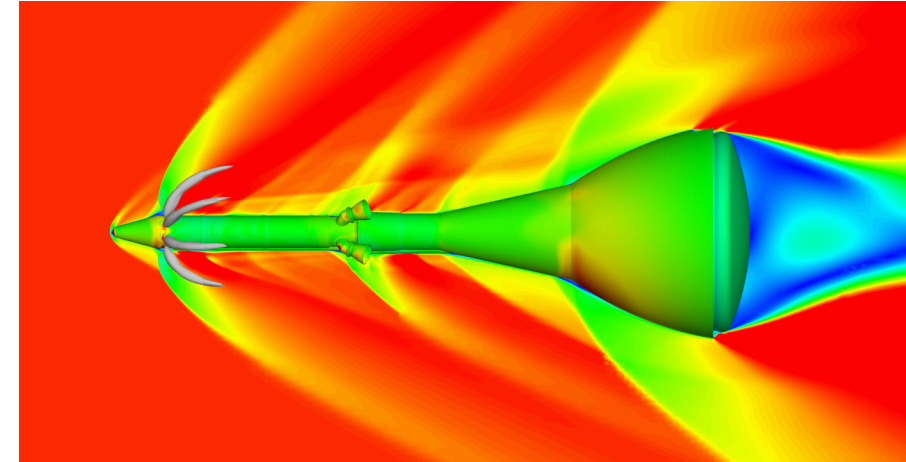
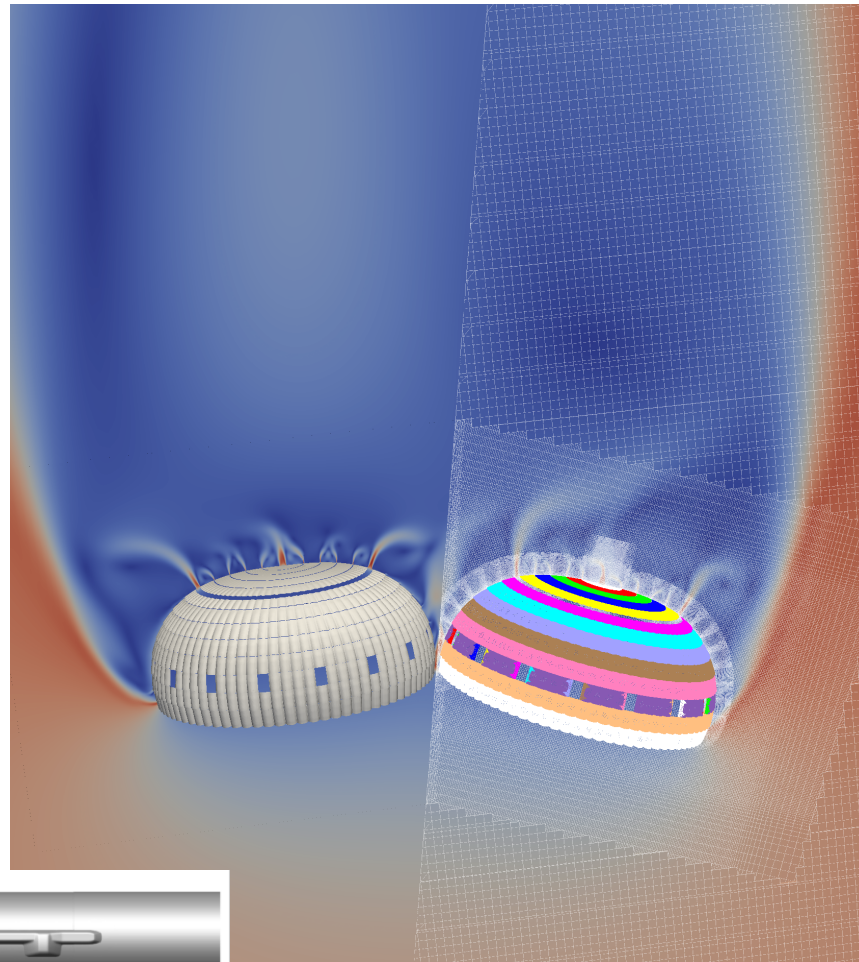
Dynamic 1-DoF Results

- Aerodynamic Model and Processing
- Comparison to Static Results

Future Work

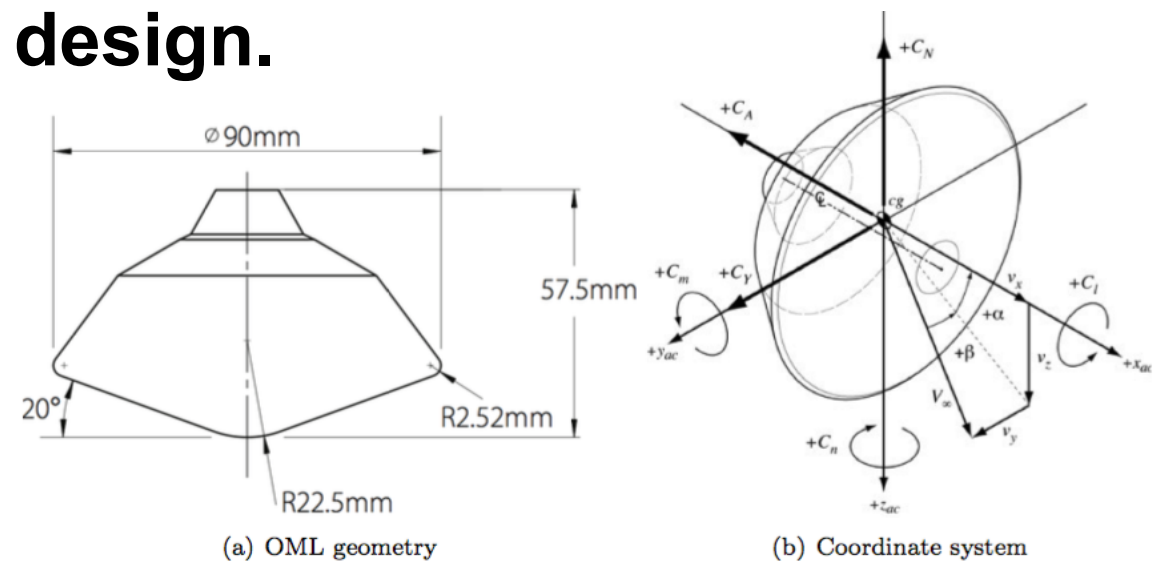
Overset techniques continue to be valuable to the work performed at JSC

- Orion
- Commercial Crew
- Red Dragon
- Propulsive Decent Technologies (a.k.a. SRP)
- **MEDLI dynamic aerodynamics**



This presentation will go into detail concerning one specific application: moving body simulations of the MSL capsule for the purpose of ballistic range test comparisons and MEDLI 2 design.

- MEDLI: Mars Science Laboratory Entry, Descent, and Landing Instrument
- MEDLI 1 was for the MSL mission.
- MEDLI 2 is for the Mars 2020 mission.



Simulations were performed using the OVERFLOW Navier-Stokes solver in support of the 90mm ballistic range test. The test was conducted earlier in 2016, but the data are still being reduced. This presentation will cover the pre-test CFD that was performed.

For dynamic simulations with a pitching capsule, overset grids were an obvious choice to enable motion of the capsule without affecting the resolution in the shock and wake.

Grid Generation

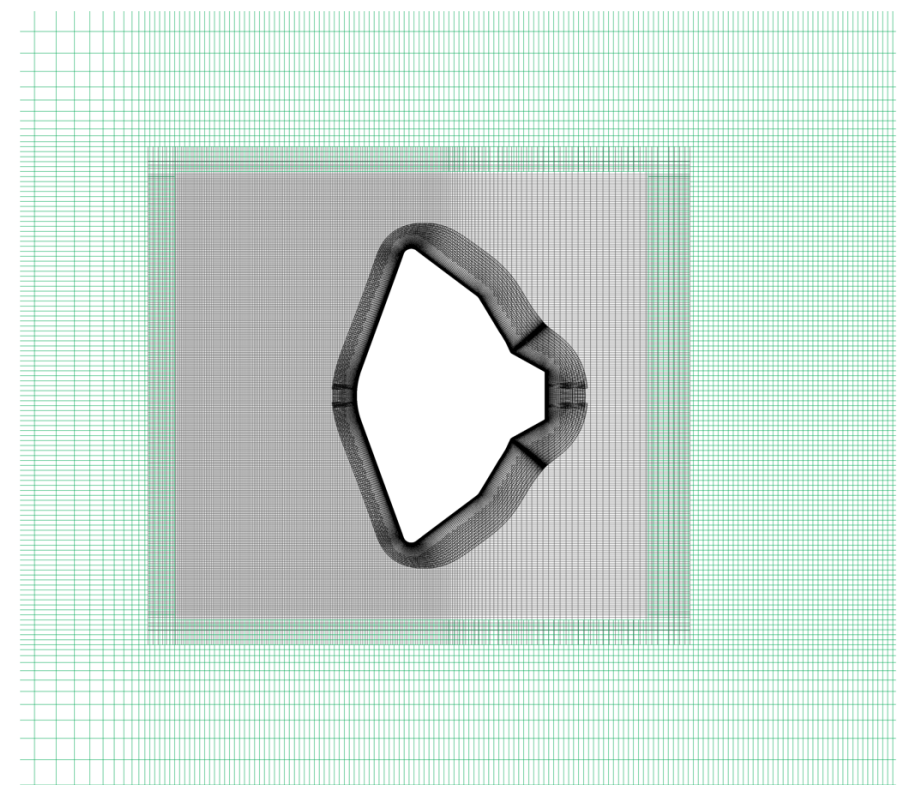
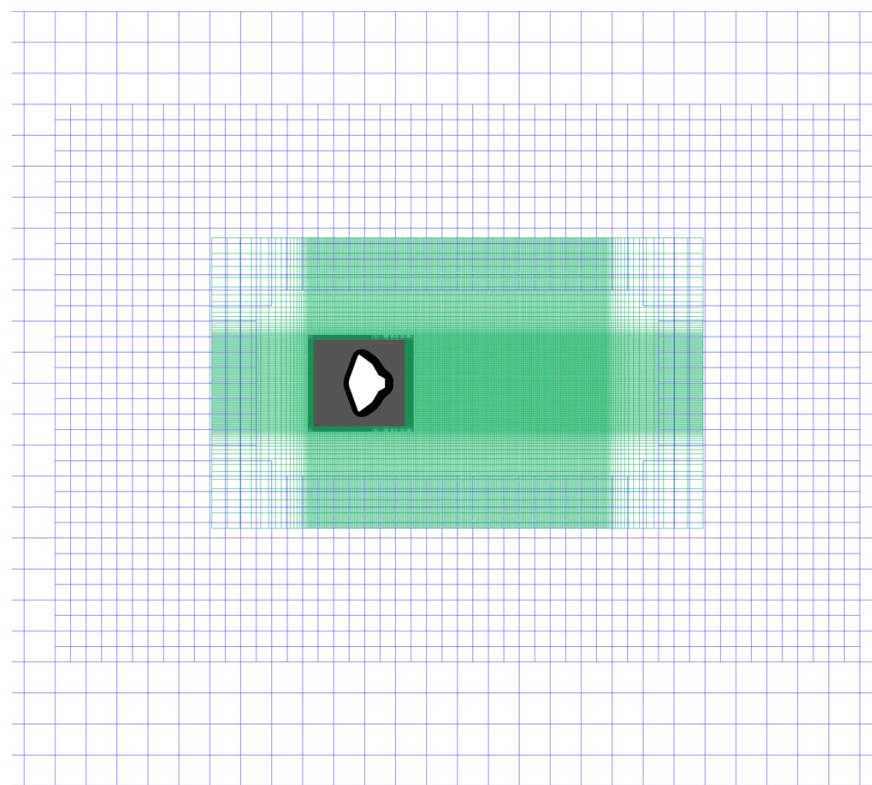
To support initial static effort and future dynamic and 6-DOF runs, a grid script system was made to enable grid motion and shock adaptation.

- Chimera Grid Tools (CGT) allow for repeatable, dynamic generation of surface and volume grids.
- Grid spacings initially based on Orion MPCV capsule grid scripts. Incorporating a decade of grid refinement studies for capsule shapes.
- Surface grid discretization was further refined to more closely match the legacy LAURA grids used by the MEDLI team.

Shock Box

Wake Box

Automatic
Off-Body Grids

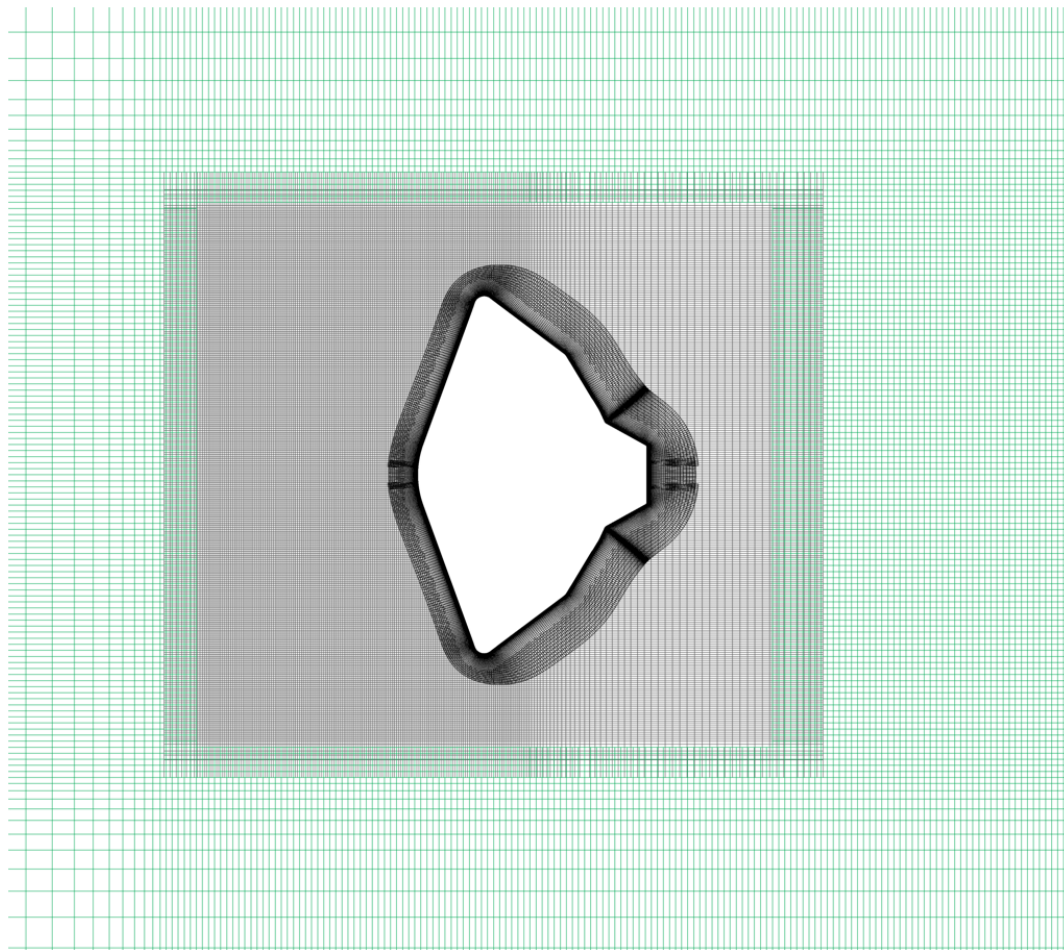


Grid Generation

OVERFLOW's build-in Domain Connectivity Function (DCF) used to perform hole cutting and interpolation for static and dynamic cases.

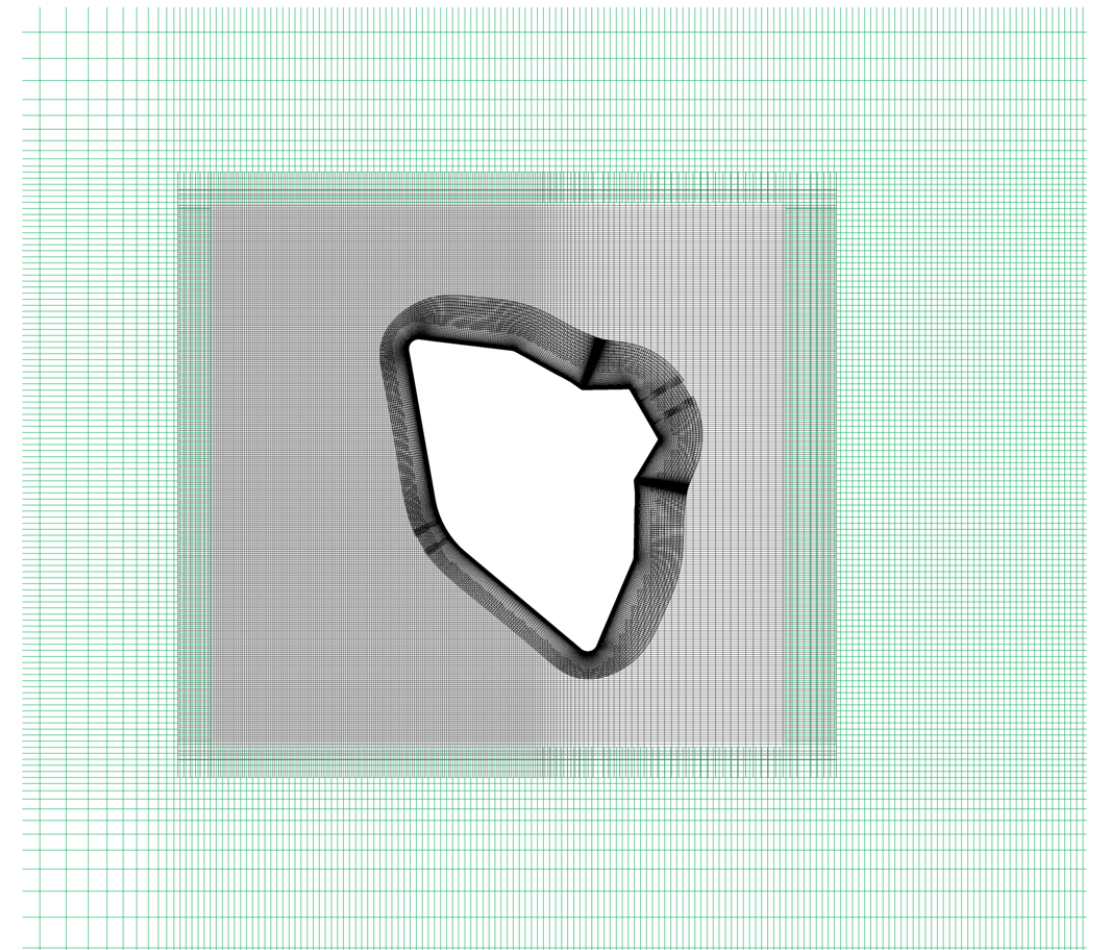
- DCF enables arbitrary orientation of capsule prior to simulation and enables moving body. It also enables automatic off-body grid generation.
- Grid is rotated about the capsule CG to vary attitude.

$\alpha = 0^\circ$



Rotation
→

$\alpha = 30^\circ$

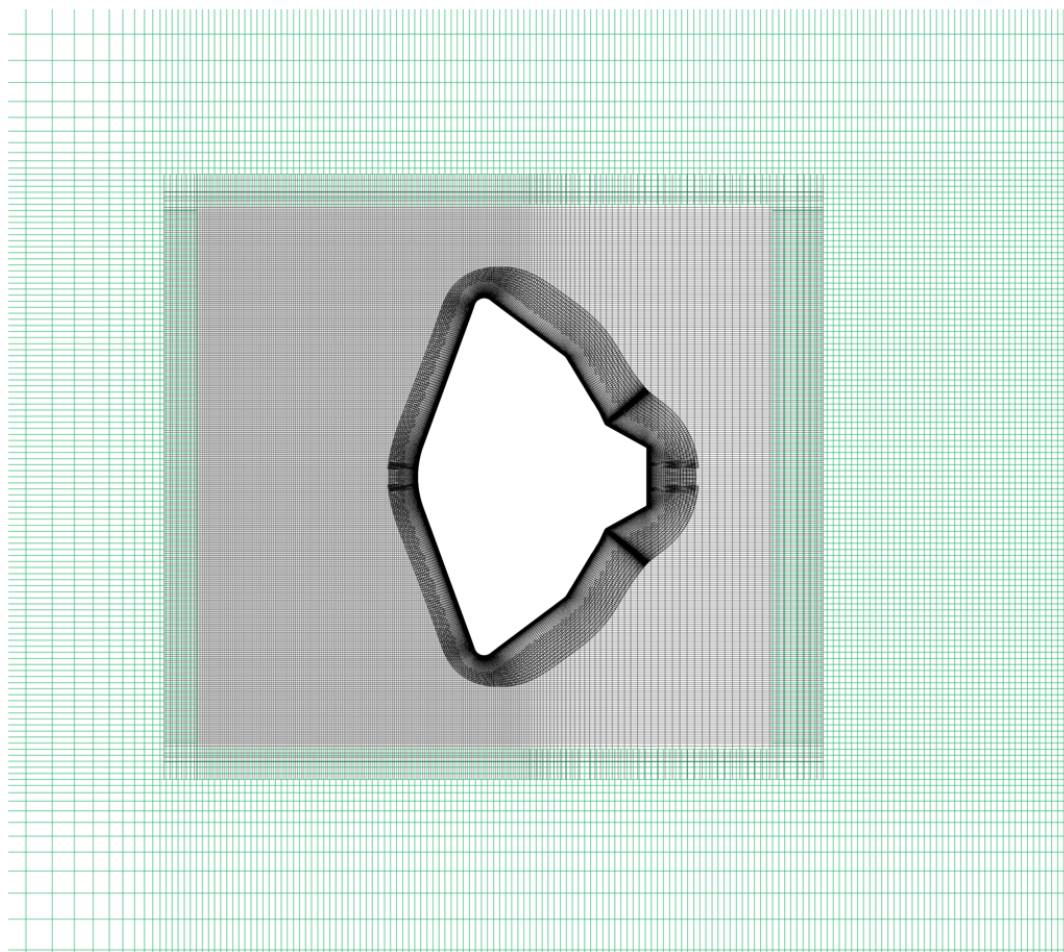


Grid Generation

OVERFLOW's build-in Domain Connectivity Function (DCF) used to perform hole cutting and interpolation for static and dynamic cases.

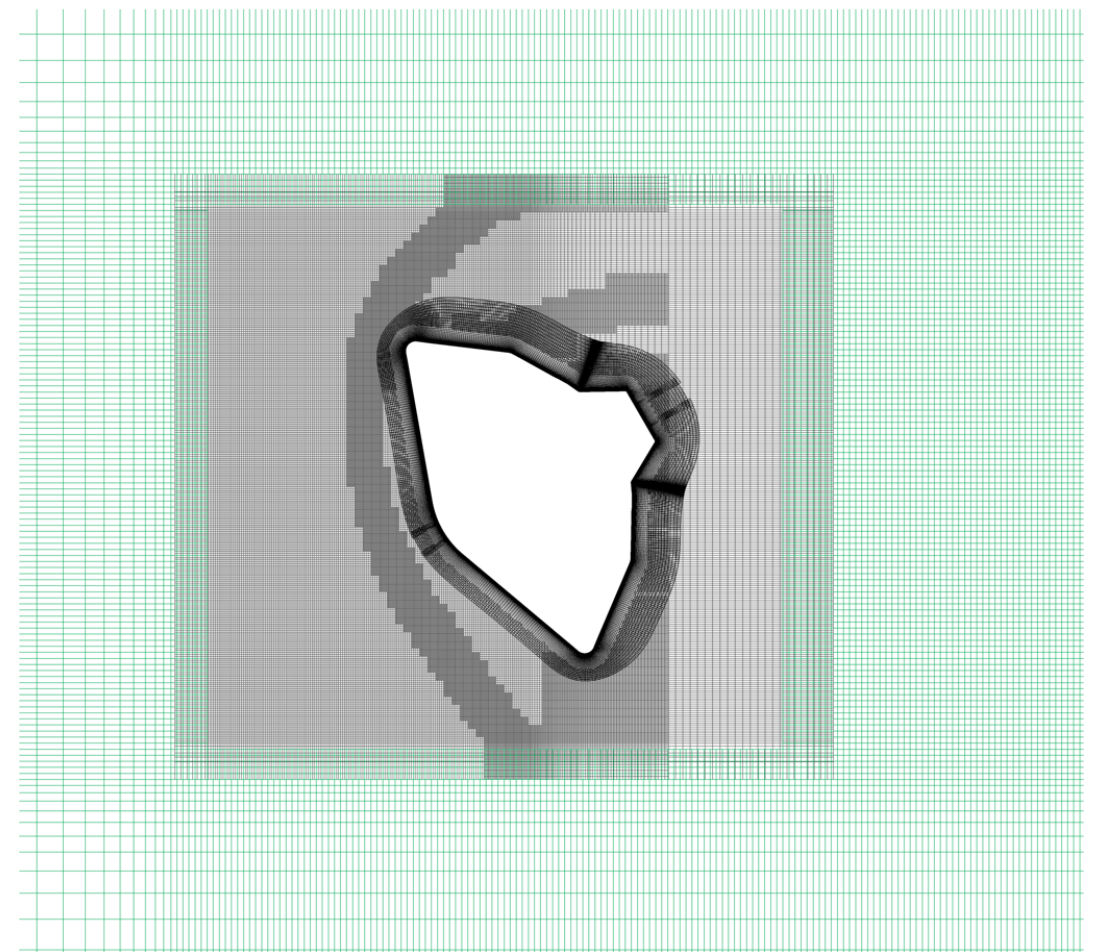
- DCF enables arbitrary orientation of capsule prior to simulation and enables moving body. It also enables automatic off-body grid generation.
- By using DCF, we were also able to use OVERFLOW's grid adaption to investigate grid sensitivity and shock resolution.

$\alpha = 0^\circ$



Rotation
→
Adaptation

$\alpha = 30^\circ$





Effects of Adaptation



Simple refinement study showed diminishing returns with grid adaptation.

- Only affect is on heatshield pressure.
- Base pressures are constant with additional refinement.

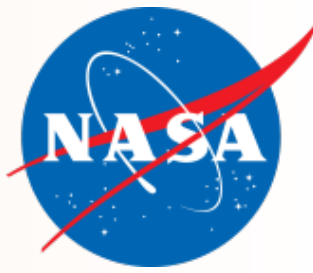
Mach 3.0 $\alpha=30^\circ$	C_A		C_N		$C_{m,x=0}$		CPU Hours (one submission)	Relative Cost
	Value	% Change	Value	% Change	Value	% Change		
Level 2	1.2739	-	-0.0917	-	0.0756	-	177	168%
Level 1	1.2723	0.13%	-0.0918	0.01%	0.0756	0.03%	147	139%
Level 0	1.2697	0.33%	-0.0914	0.40%	0.0753	0.37%	106	100%

One level of adaption was used for the static simulations. No adaptation was used for the dynamic simulations.

- Not used for dynamic simulations in order to minimize cost since benefit was small.
- Shock box spacing is 0.0056D, 0.0028D in regions of adaption.



OVERFLOW Inputs



Simulations use OVERFLOW version 2.2k.

- Turbulent, viscous Navier-Stokes solver
- Using SST-DES turbulence model (NQT=205, IDES=1)
- Using HLLE++ numerical fluxes (IRHS=6, DELTA=5.0)
- Implicit SSOR time advancement (ILHS=6)
- Adaptation on undivided differences (ETYPE=0, MAX_SIZE=80.e6)
- Time-accurate, unsteady flow (DTPHYS=0.04, NITNWT=4-8)
 - Sensitivity study was performed to determine the timestep.
 - Cases show 3-4 orders of magnitude drop in average residual during sub-iterations.
- Viscous, Isothermal wall temperature of 540 °R

At JSC, we have developed an OVERFLOW run manager, `overlst`.

- It is a collection of Perl modules that interface with CGT and OVERFLOW as well as several compute clusters.
- Relevant portions have been augmented to handle DCF and moving body simulations.
- This run manager handled the nearly 100 preliminary, static, and dynamic simulations used for this work.

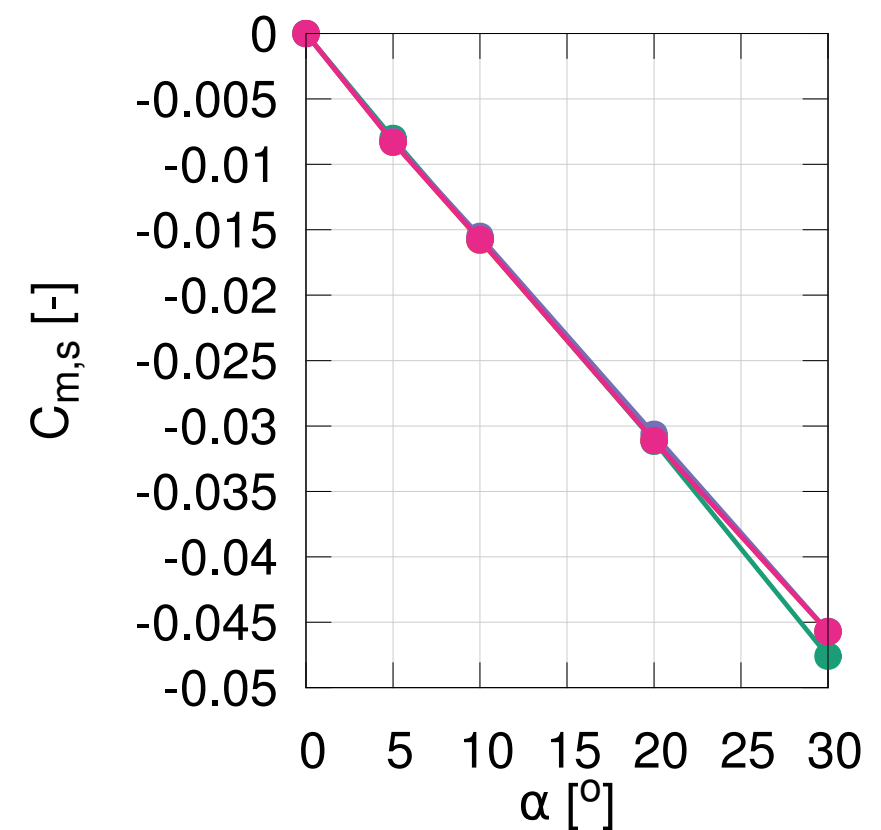
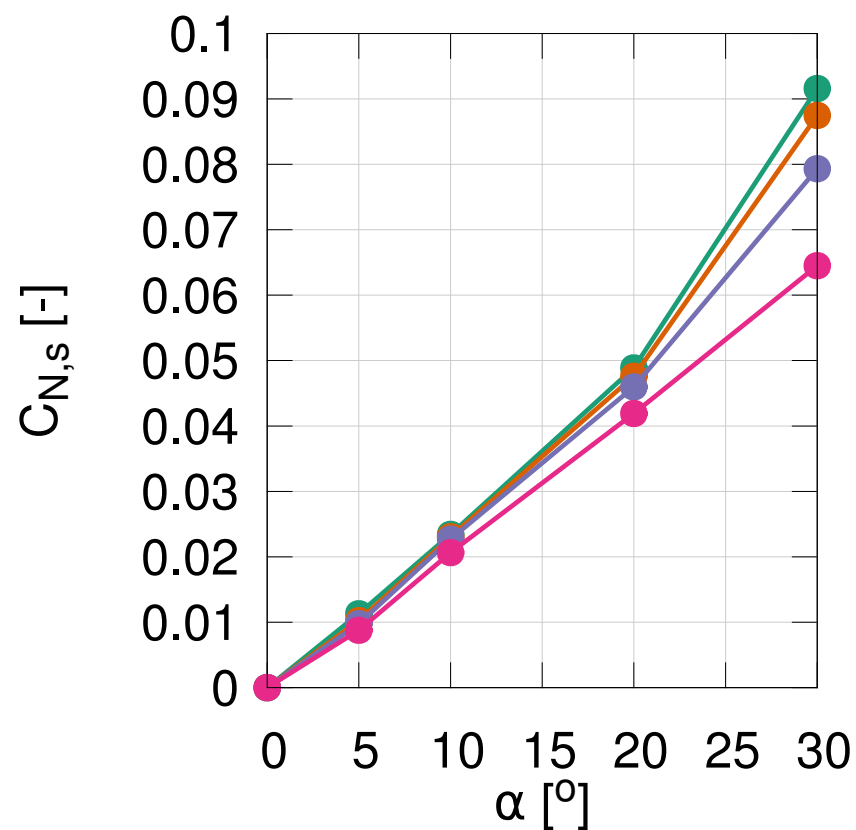
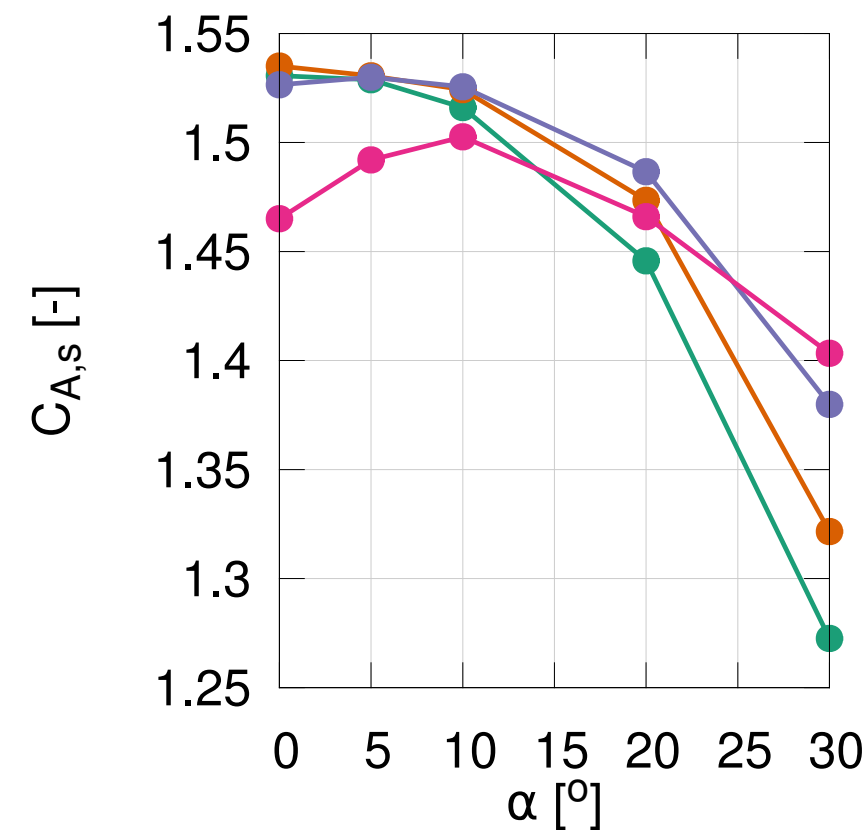
Static aerodynamics were integrated from static simulations:

- Sea level conditions (simulating ballistic range)
- Mach numbers considered: 1.5, 2.0, 2.5, 3.0
- $0^\circ < \alpha < 30^\circ$

Goal was to develop static aerodynamic curves to compare to existing models and the future dynamic work.

- Mach 1.5 reduction in axial force at low α corroborated by other sources.

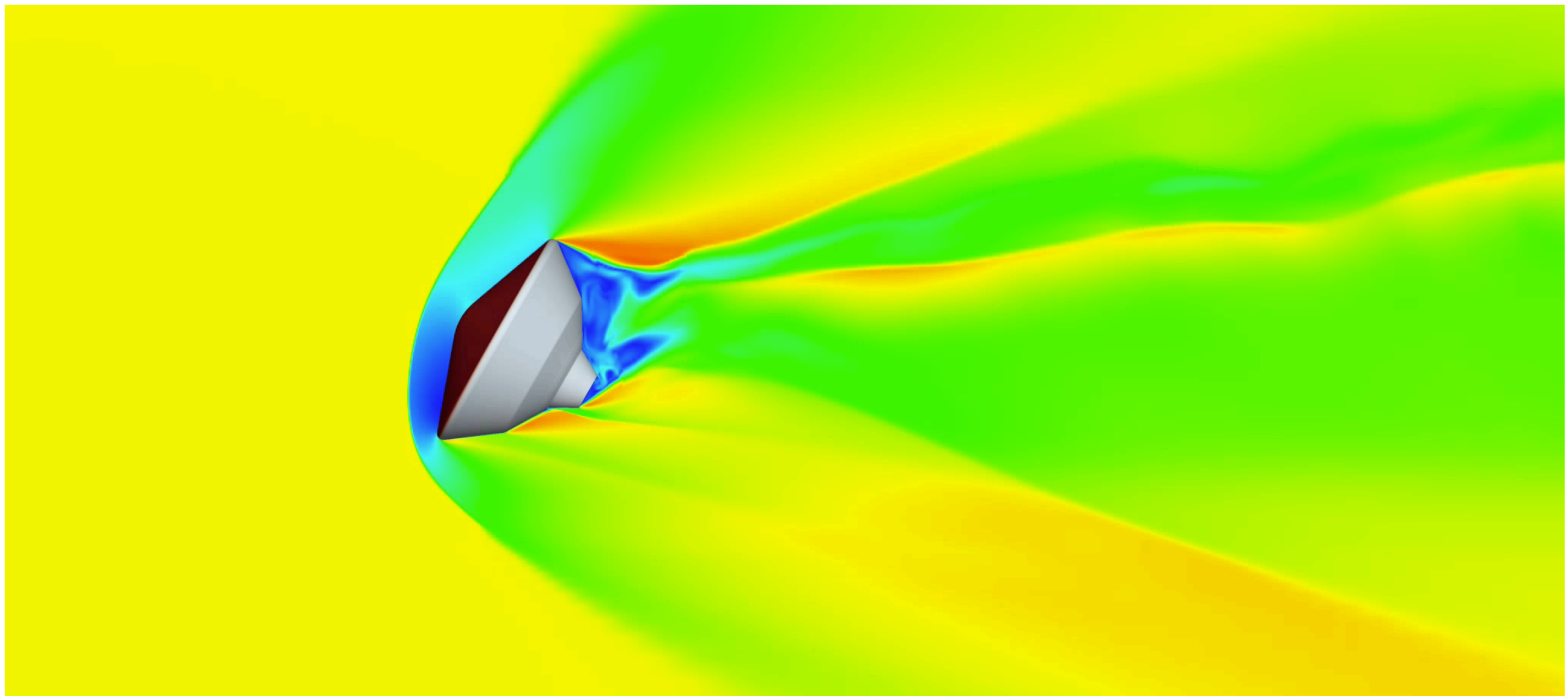
Mach 3.0 ● Mach 2.5 ● Mach 2.0 ● Mach 1.5 ●



1-DoF simulations were performed looking at pitch damping from an initially static MSL at varying angle of attack.

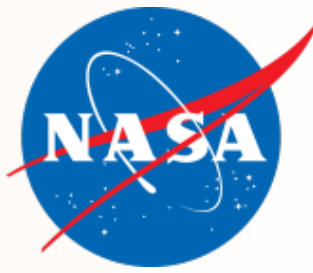
- Initial amplitudes of 5° , 10° , 15° , and 30° at Mach 1.5 and 3.0
- Same conditions and numerics used previously, but no adaptation.

Mach contours from case initially at 30° .





Aerodynamic Model



Assume linear response in dynamic derivatives with respect to pitch-rate (q) and that dynamic derivatives are only a function of α and not q .

- Based on the data, there is evidence of non-linearity in dynamic derivatives.

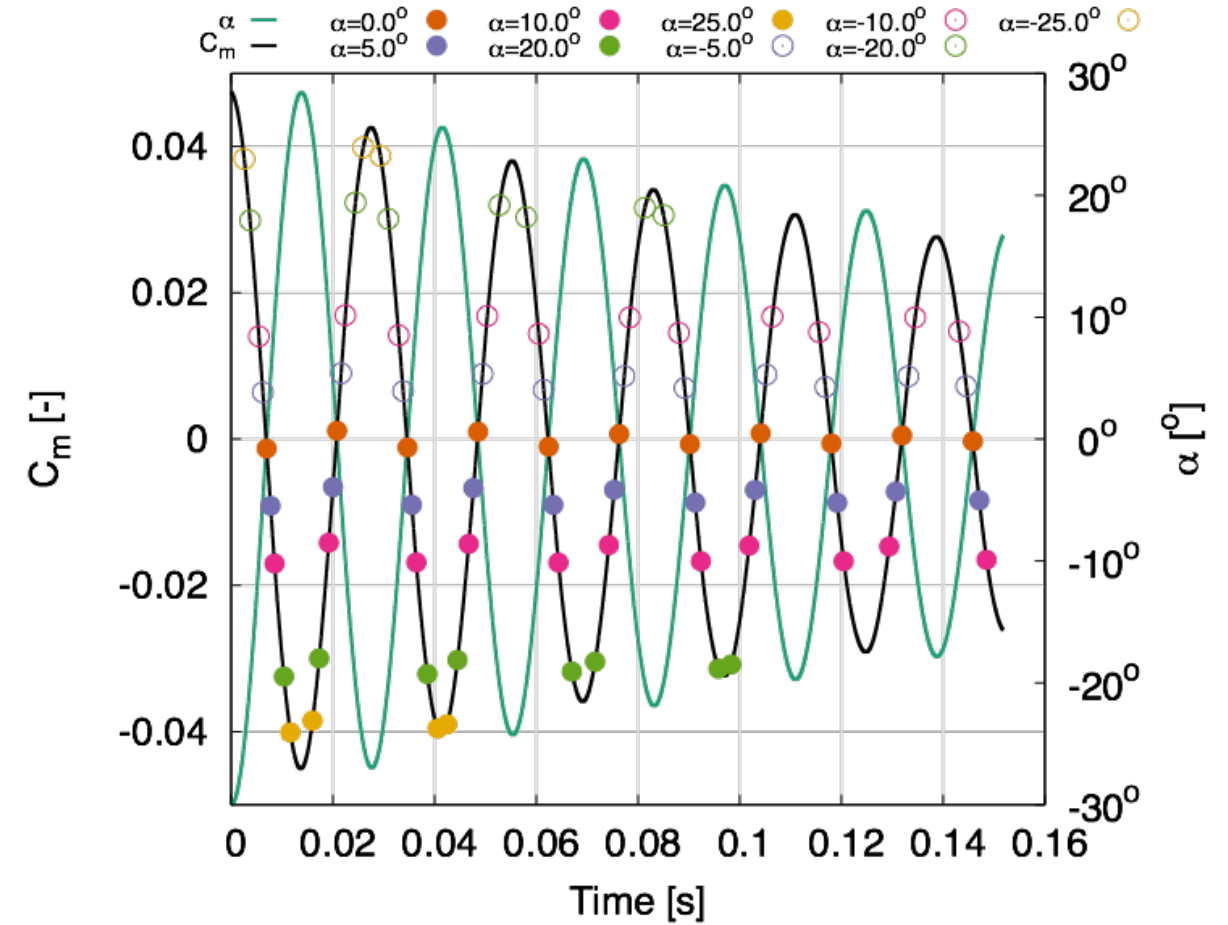
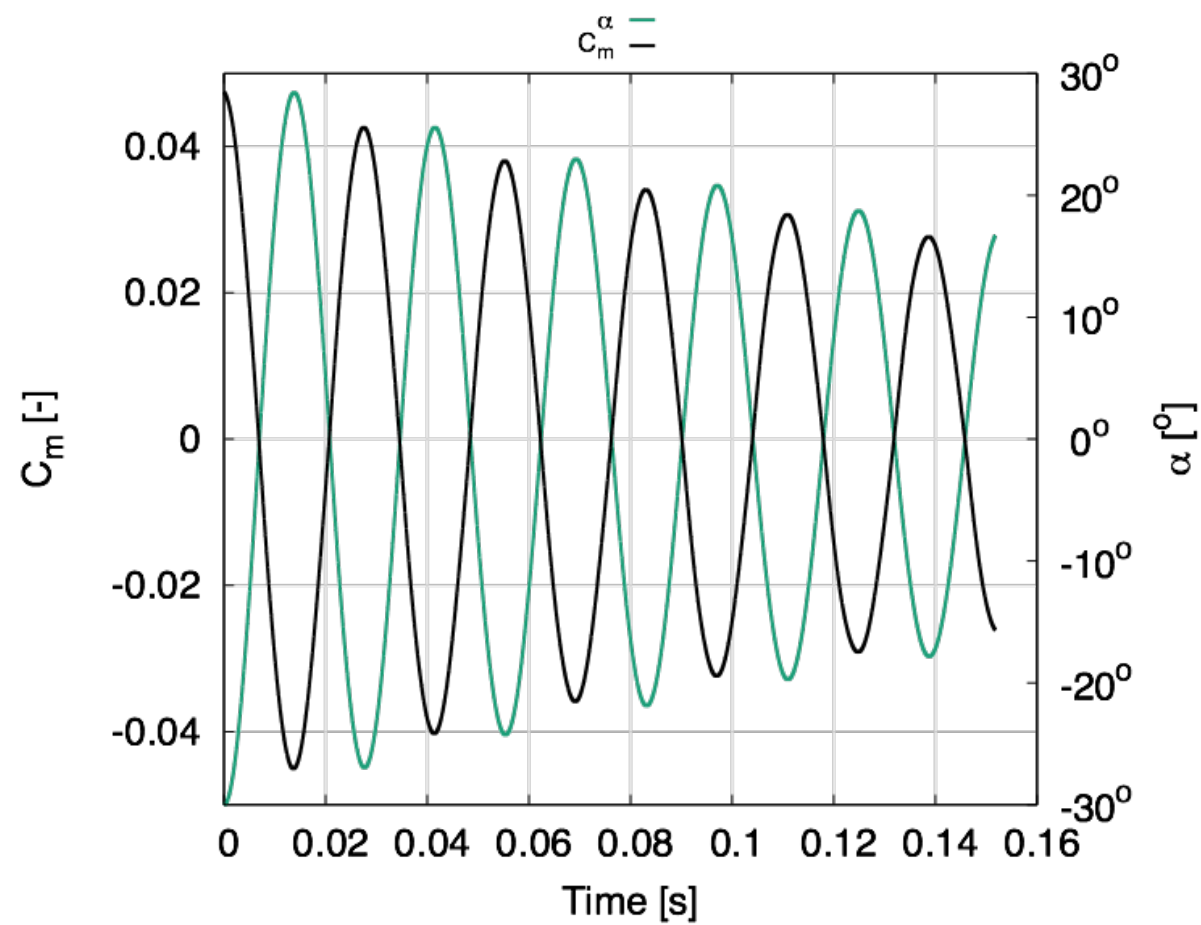
$$C_{\phi} = \underbrace{C_{\phi}(\alpha)}_{static} + \underbrace{C_{\phi,q}(\alpha)}_{dynamic} \times q$$

Based on the above, the dynamic simulations can be used to get estimates of static and dynamic aerodynamic coefficients.

- Least-squares fit through available data at angles of attack.
- Details are shown on following slides.

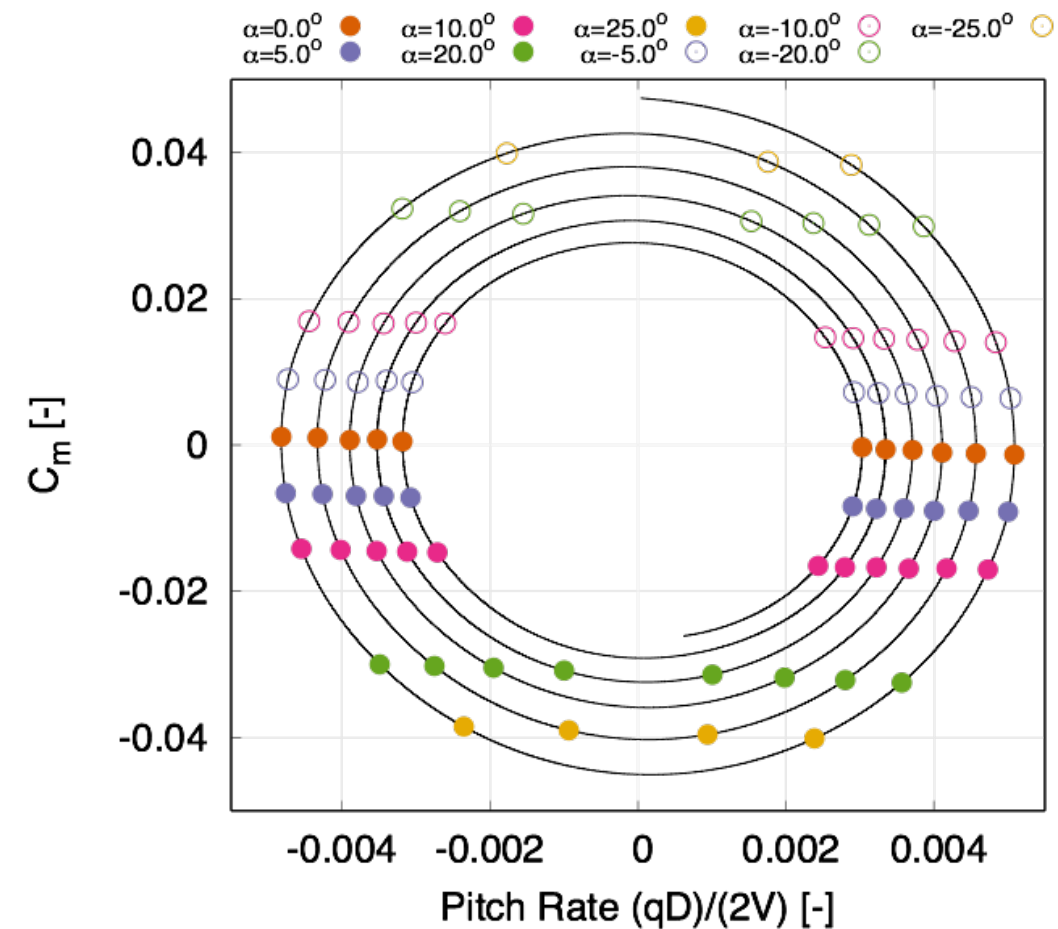
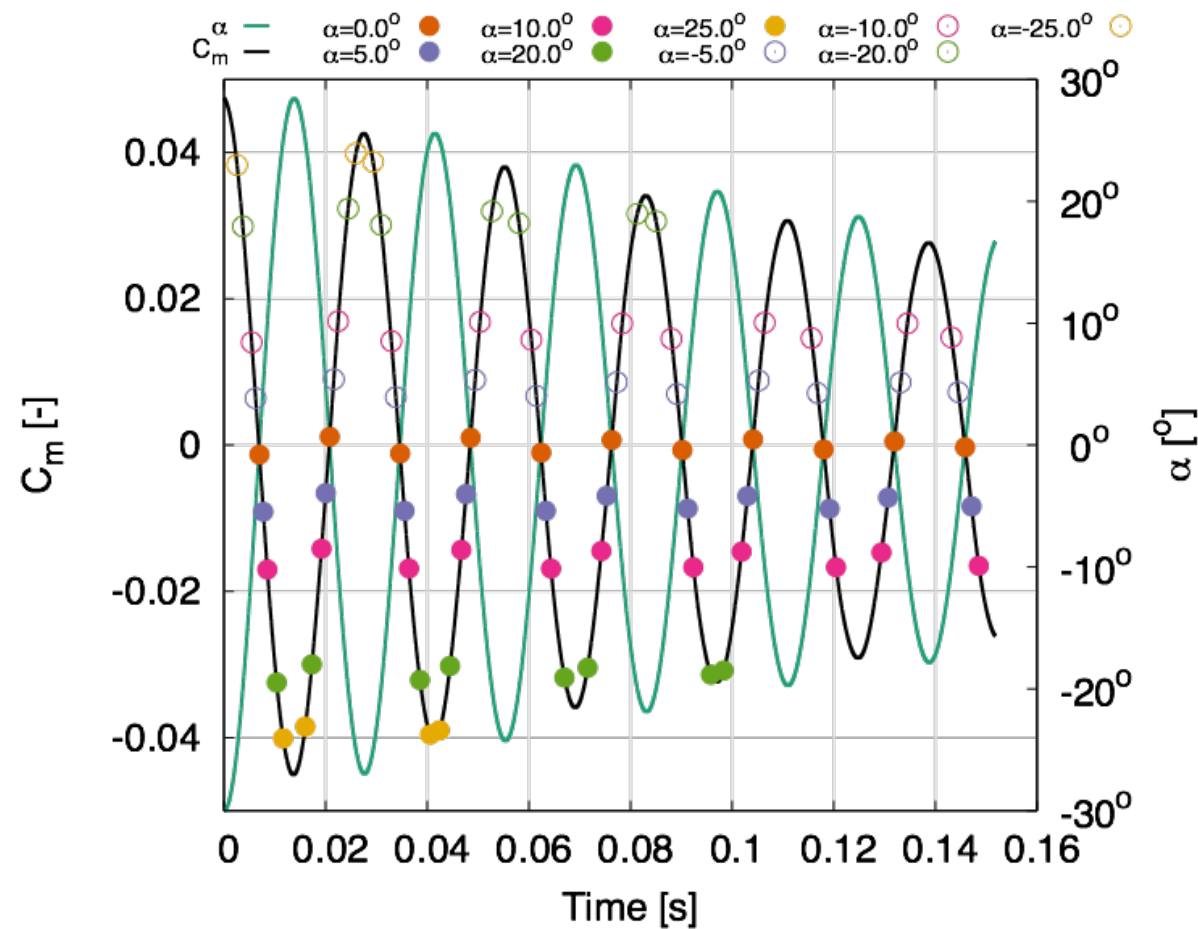
Run strategy begins with converged static simulation and then allows motion.

- First half period of oscillation thrown out to eliminate effect of transients.



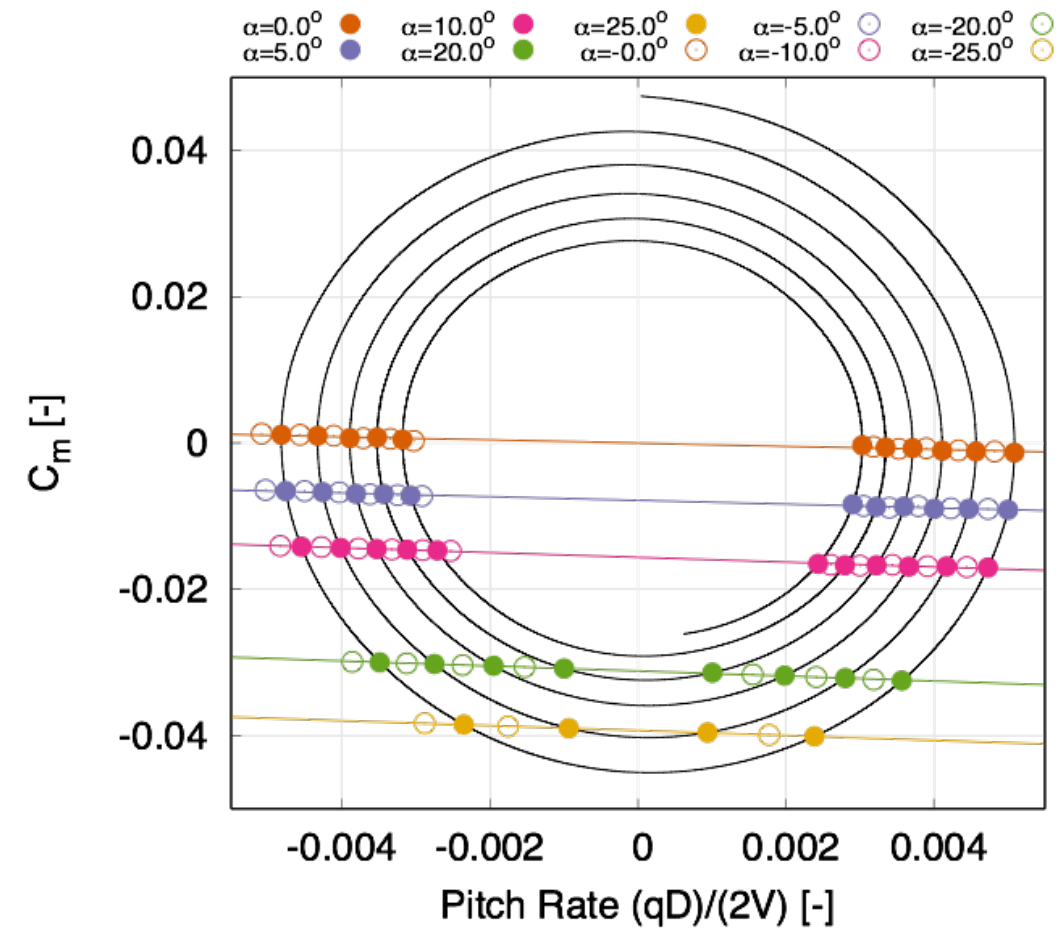
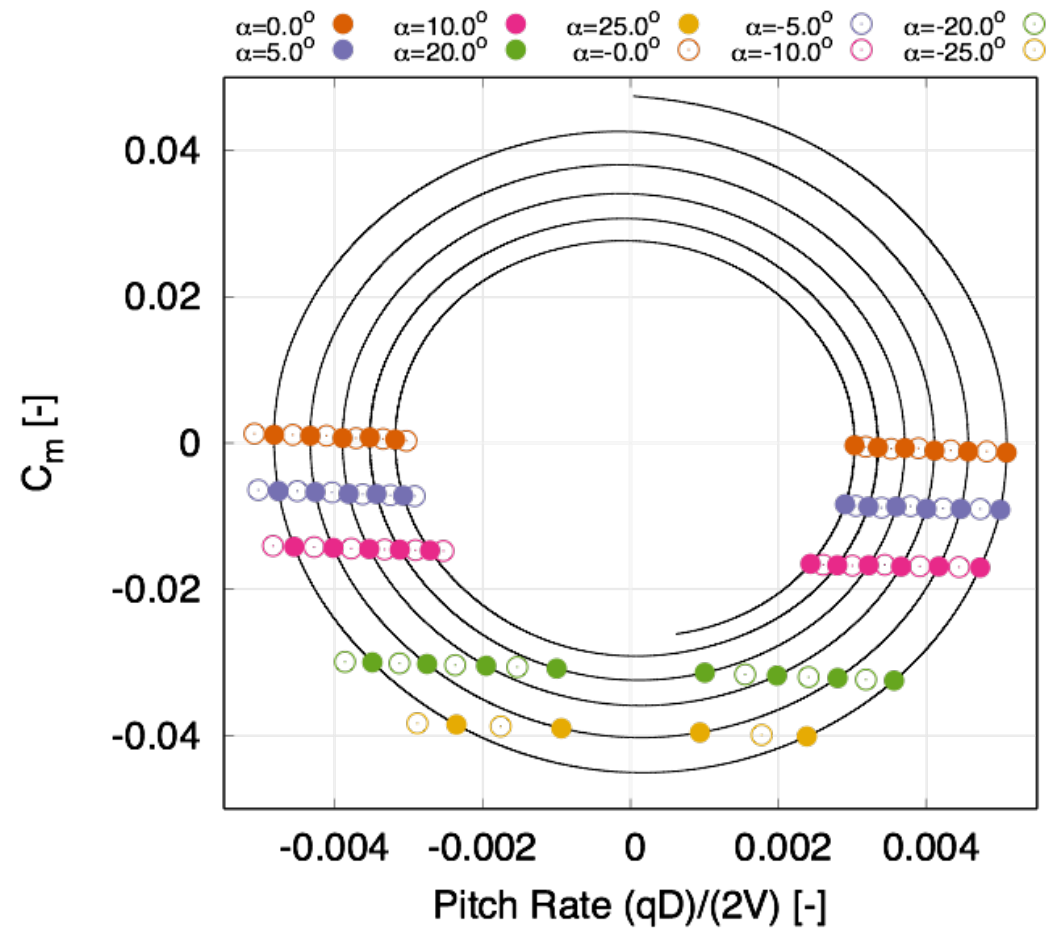
From time history of aerodynamics and angle of attack, identify all points at a discrete angle of attack.

- Increments of 0.5° were used to discretize attitude.



For visualization, these data can be replotted versus pitch rate.

- Inherent symmetry in the geometry and problem allow for mirroring all data at negative α to increase the effective number of points at positive α .

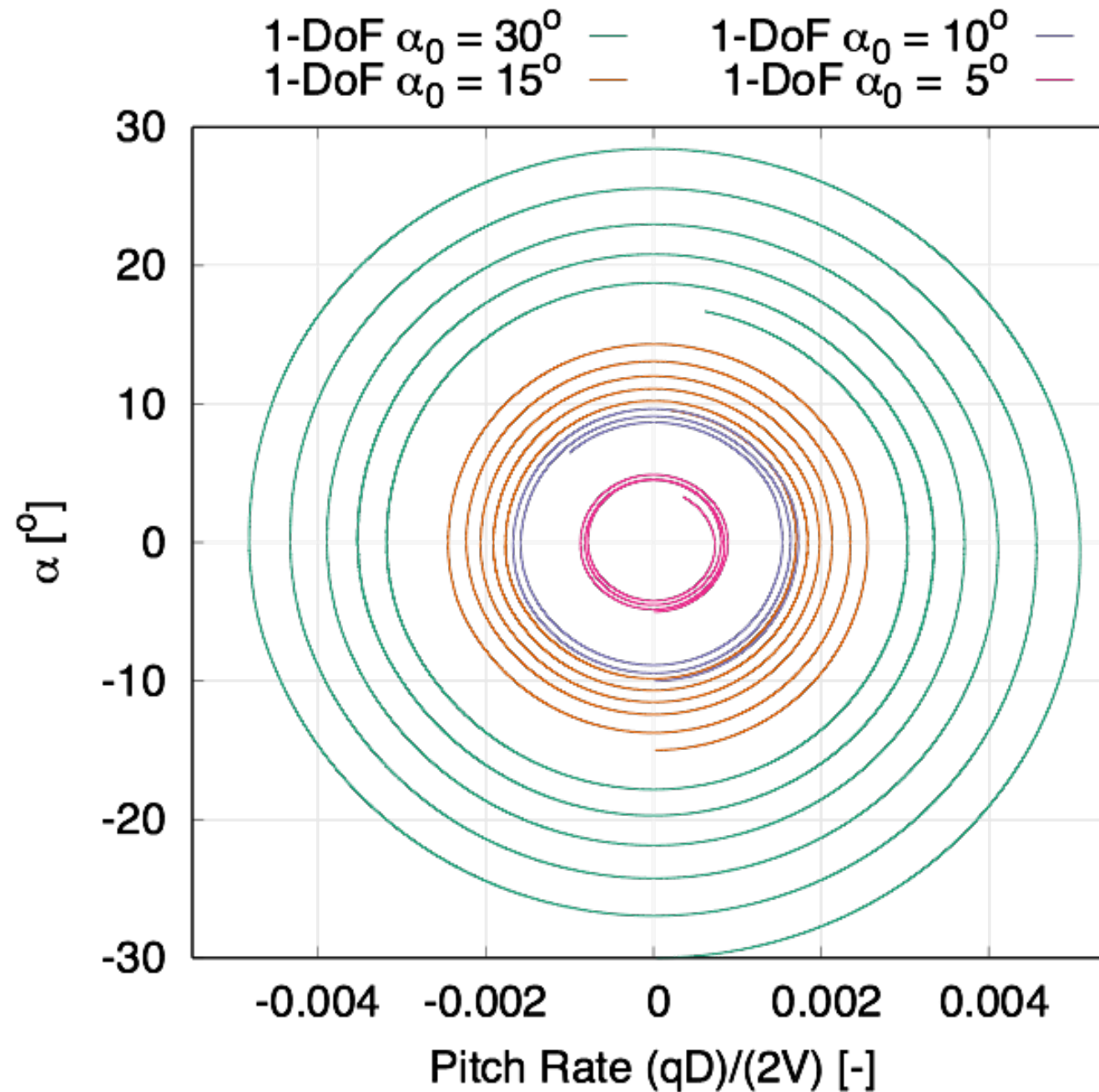


For visualization, these data can be replotted versus pitch rate.

$$C_{\phi} = \underbrace{C_{\phi}(\alpha)}_b + \underbrace{C_{\phi,q}(\alpha) \times q}_{mx}$$

Slope of resulting least-squares fit is $C_{\phi,q}(\alpha)$; intercept is $C_{\phi}(\alpha)$.

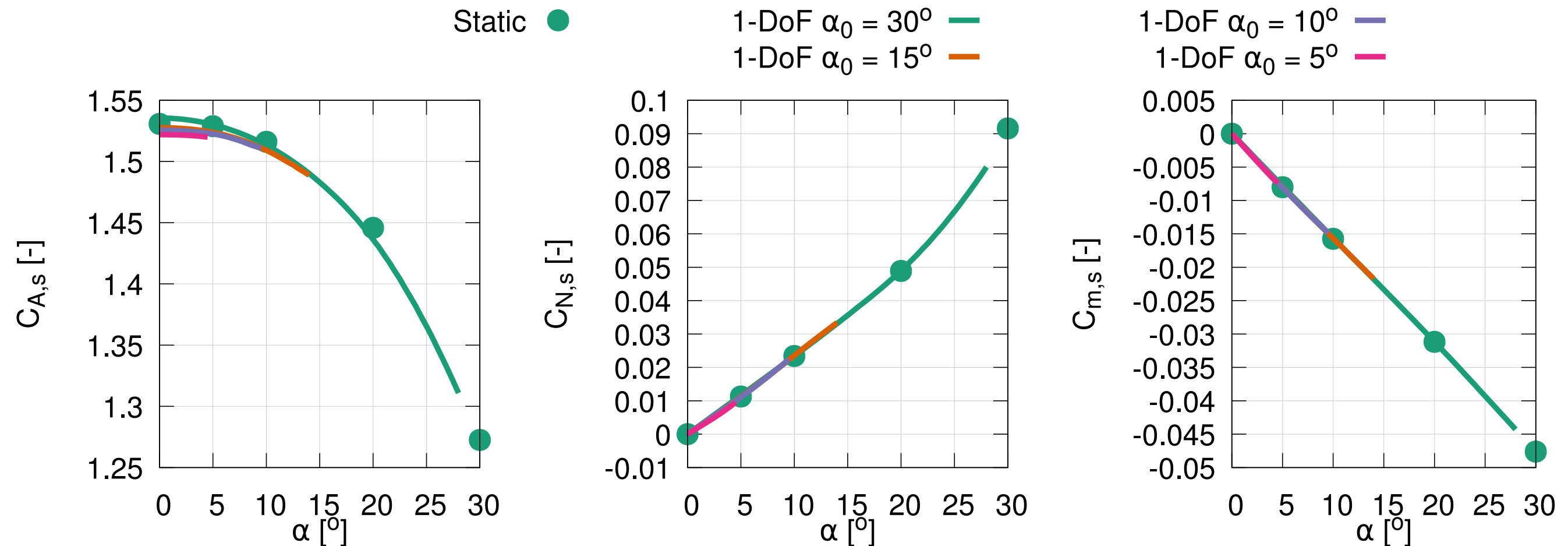
Varying the initial pitch amplitude affects the pitch rates that are observed at a given α . If $C_{m,q}$ is linear as the model assumes and only a function of α and extracted aerodynamics from all four simulations should agree.



To assess the validity of the method, we compare static aerodynamic coefficients from the static simulations to the static coefficients calculated with the curve fit of the dynamic simulations.

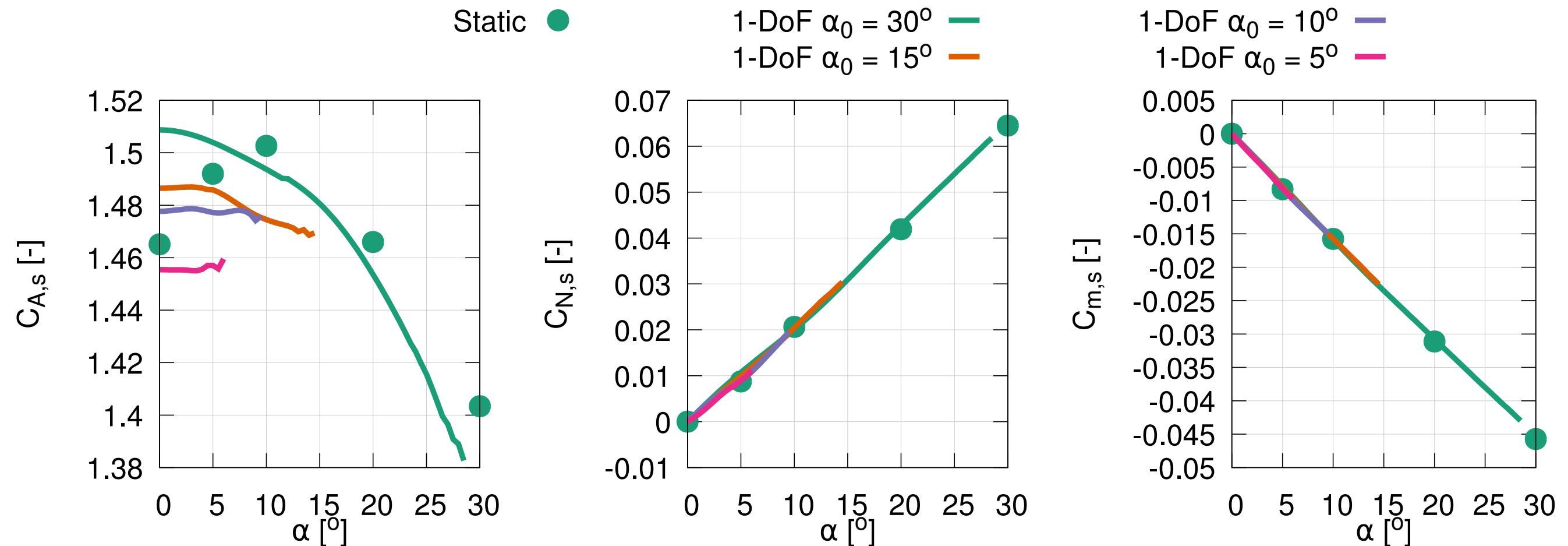
Mach 3.0:

- Fit with the 30° data compares very well to the static results from earlier.
- Fit with other angles is comparable, but noticeable deviations in $C_{A,s}$ (non-linear?).



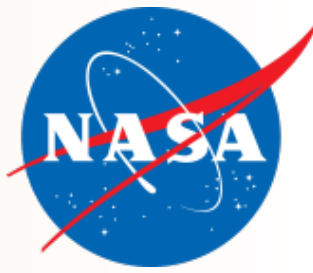
Mach 1.5:

- Only three cycles of motion versus six at Mach 3.0. Lower speed, generally more difficult and less stable. 5° simulation is noticeably undamped.
- Data from moving simulations not as smooth as for Mach 3.0. $C_{A,s}$ shows larger deviations. For $C_{N,s}$ and $C_{m,s}$ the agreement is still good between static and dynamic simulations.





Results - Dynamic Simulations



A ballistic range test was preformed for the MSL capsule ~10 years ago.

- It was performed at a different scale as compared to the current work (65mm versus 90mm) and has slightly different mass properties.
- Ballistic range reductions for dynamic terms are quite different than the linear model and curve-fit that was shown previously. Portions of several runs are combined and data are fit using multiple coefficients.

$$C_{m_q} = C_{m_q,initial} + C_{m_q,2}\varepsilon^2 + C_{m_q,4}\varepsilon^4 + C_{m_q,m}(M_i - M_{ref}) + C_{m_q,m2}(M_i - M_{ref})^2$$

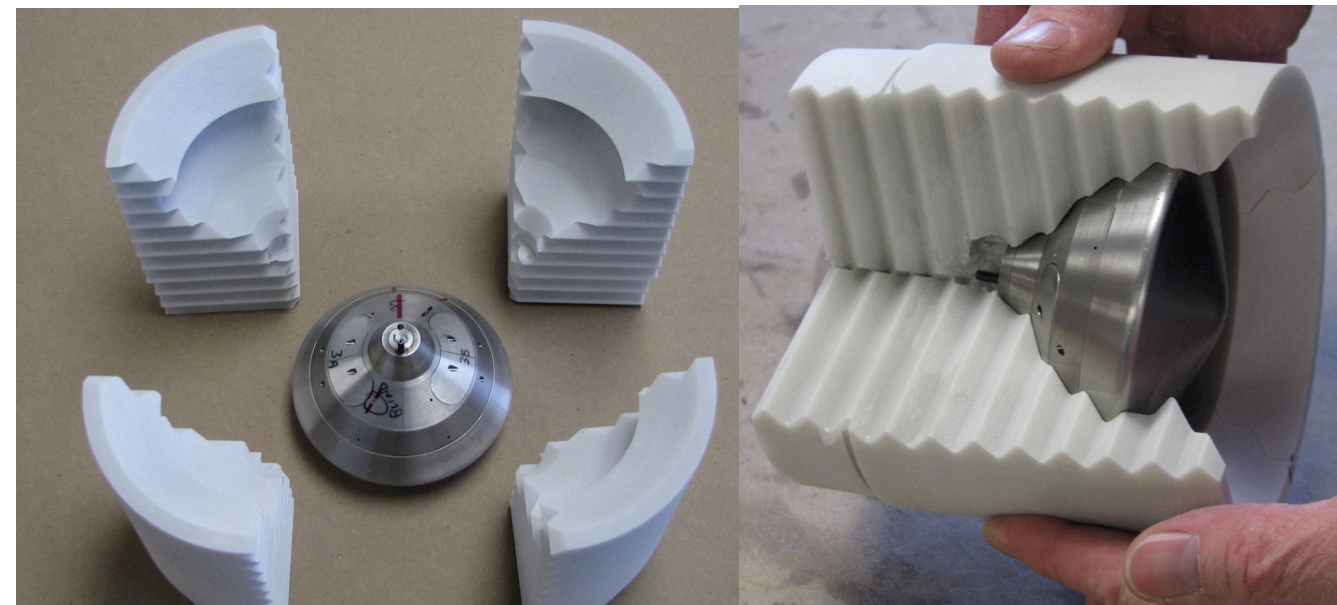
$$\varepsilon = \sin(\alpha_T) = \sqrt{\frac{V_z^2 + V_y^2}{V^2}}$$

$$M_{ref} = 2.5$$

- Regardless, our hope was that this data could give us an order of magnitude comparison to the CFD.
- Data taken from AIAA 2009-3917: “Dynamic Stability Testing of the Mars Science Laboratory Entry Capsule”

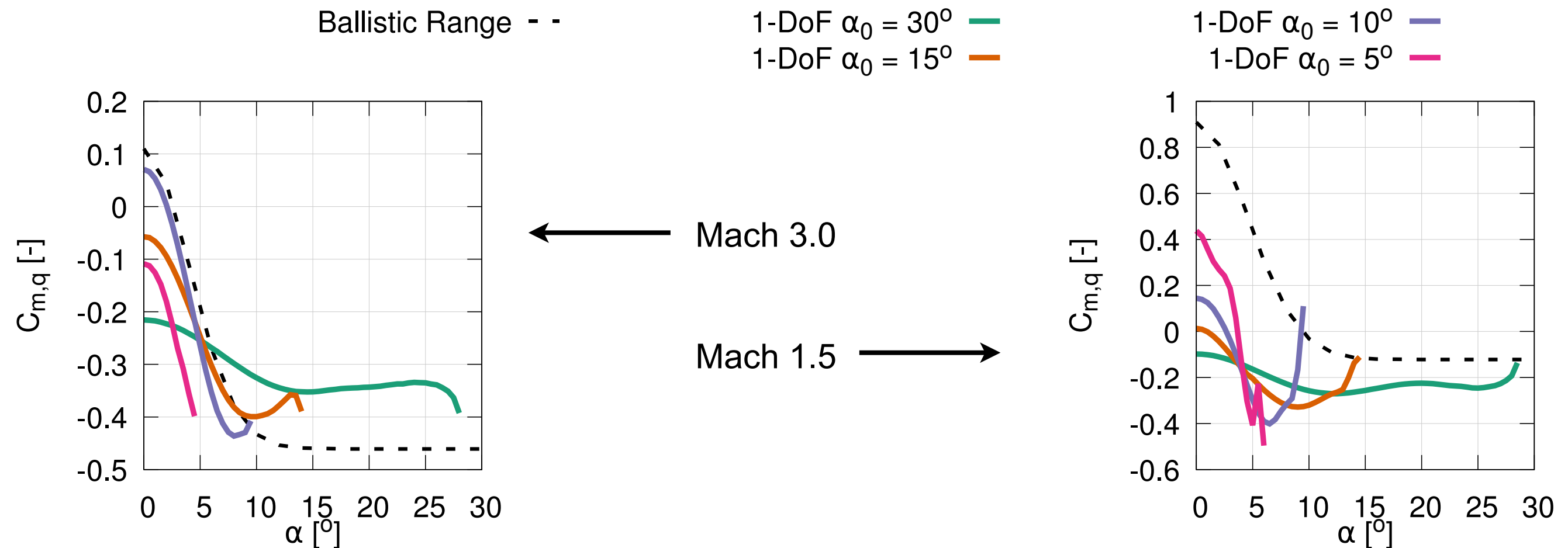
A ballistic range test includes placing a scale model inside of a sabot at a desired initial orientation. The sabot and model are placed into a gun and fired down an instrumented range.

- Onboard instrumentation
- Photogrammetry stations



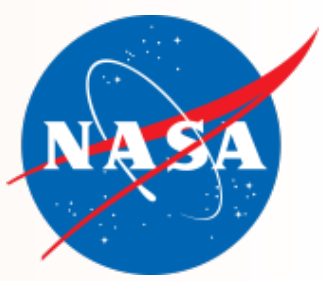
Order of magnitude is similar. Some observations:

- Variation in the results from the simulations imply that our model is not perfect or that $C_{m,q}$ is also a function of pitch rate.
- At Mach 3.0, the data shows good agreement with the range data using the data from the 10° and 15° simulations.
- Mach 1.5 show a reduction in damping as compared to Mach 3.0 . Do not agree as well with the range data.





Conclusion and Future Work



Ability to couple CGT grid scripts and OVERFLOW DCF was crucial to enable rapid development of grids and solutions.

Method with rotating body-fitted, viscous grids showed agreement with static data and similarity with previous ballistic range data.

Entire process (static, dynamic, reduction, and comparison) performed with non-overset solver (US3D) and agreement was very good.

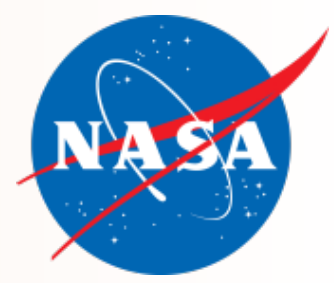
- More details can be found in conference paper:
‘Dynamic CFD Simulations of the MEADS II Ballistic Range Test Model’ (AIAA 2016-3243)

2016 ballistic range data is currently being reduced for additional runs.

- New cases being run to match the range conditions.
- Plan is to perform 1-DoF prescribed and 6-DoF free simulations for comparison using OVERFLOW.
- Data reduction strategy will be augmented to include method used in the ballistic range tests.



Backup



Grids system and inputs for OVERFLOW updated to allow for 6-DOF or prescribed motion input.

Mass Properties for model:

- $I_x = 916460.86 \text{ [g*mm}^2\text{]}$
- $I_y = 619454.59 \text{ [g*mm}^2\text{]}$
- $I_z = 656597.73 \text{ [g*mm}^2\text{]}$
- Mass = 1369.76 [g]
- $(X, Y, Z)_{CG} = (-0.3002D, 0.0, 0.0)$

Simplified for initial work to:

- $I_x = 916000 \text{ [g*mm}^2\text{]}$
- $I_y = 638000 \text{ [g*mm}^2\text{]}$
- $I_z = 638000 \text{ [g*mm}^2\text{]}$
- Mass = 1370 [g]

